frontiers | Frontiers in Physics

TYPE Original Research
PUBLISHED 17 August 2023
DOI 10.3389/fphy.2023.1191954

OPEN ACCESS

EDITED BY
Digesh Raut,
Washington College, United States

REVIEWED BY
Ge Yang,
North Carolina State University,
United States
Atanu Pathak,
Purdue University Northwest,
United States
Peter R. Hobson,
Queen Mary University of London,
United Kingdom

*CORRESPONDENCE
César Jesús-Valls,
cesar.jesus-valls@ipmu.jp
Federico Sánchez,
federico.sancheznieto@unige.ch

RECEIVED 22 March 2023
ACCEPTED 18 July 2023
PUBLISHED 17 August 2023

CITATION
Jesús-Valls C and Sánchez F (2023), Lead perovskites as CEνNS detectors.
Front. Phys. 11:1191954.
doi: 10.3389/fphy.2023.1191954

Lead perovskites as CEνNS detectors

César Jesús-Valls[1]* and Federico Sánchez[2]*

[1]Kavli Institute for the Physics and Mathematics of the Universe (WPI), University of Tokyo Institutes for Advanced Study, University of Tokyo, Kashiwa, Japan, [2]Section de Physique, University of Geneva, Geneva, Switzerland

Introduction: The recent discovery of coherent elastic neutrino-nucleus scattering (CEvNS) has created new opportunities to detect and study neutrinos. The interaction cross section in CEvNS scales quadratically with the number of neutrons, making heavy-nuclei targets such as active lead-based detectors ideal. Lead perovskites have emerged in the last decade as revolutionary materials for radiation detection due to their heavy and flexible element composition and their unique optoelectronic properties that result in an excellent energy resolution at an economic cost.

Methodology: In this study, we discuss, for the first time, the physics potential and feasibility of building neutrino detectors using semiconductor lead perovskite crystals as a target.

Results and Discussion: We indicate that existing data with x-rays suggest the suitability of existing lead perovskite sensors to study CEvNS using neutrinos from π decay at rest (π- DAR) sources. Although dedicated research and development will be necessary, we have found significant benefits and no inherent obstacles for the development of lead perovskites as CEvNS detectors.

KEYWORDS

neutrino, nuclear coherent scattering, perovskites, novel detectors, low-energy interactions

1 Introduction

Neutrinos are the only known fermions carrying exclusively weak charges and, therefore, are clean probes of the weak interaction and unique messengers of dense matter environments, unaffected by strong and electromagnetic interactions. These appeals, however, result in notably suppressed interaction cross sections, hampering the study of neutrino physics and rendering most applications impractical.

In 1974, the existence of coherent elastic neutrino-nucleus scattering (CEνNS) was pointed out as a consequence of the standard model [1]. In CEνNS, a neutrino transfers momentum to a whole nucleus via the exchange of a virtual Z boson, forcing it to recoil. The interaction cross section for this process is

$$\frac{d\sigma^{\mathrm{CE\nu NS}}}{dE_R} = \frac{G_F^2}{8\pi\cdot(\hbar c)^4}\left(N + \left(1 - 4\sin^2\theta_W\right)Z\right)^2 \cdot m_N \cdot \left(2 - E_R m_N/E_\nu^2\right)|f(q)|^2 \tag{1}$$

where G_F is the Fermi constant, N (Z) is the number of neutrons (protons), θ_W is the Weinberg angle, and m_N and E_R are the nucleon mass and its recoil energy, respectively. The nuclear form factor $f(q)$ characterizes the loss of coherence as a function of the transferred momentum $q = \sqrt{2m_N E_R}/\hbar$, and it is close to unity for small q, associated with typical neutrino energies $E_\nu \lesssim$

50 MeV. Notably, given that $4\sin^2\theta_W \sim 1$, $\sigma^{\mathrm{CE}\nu\mathrm{NS}} \propto N^2$ [2]. This remarkable interaction cross section enhancement, however, offers a very challenging detection signal as the nucleon recoil needs to be identified. The maximum recoil energy scales as $E_R^{\max} \approx 2E_\nu^2/m_N$ so that detectors need to be able to measure recoil energies of, at most, several tens of keV. Thanks to recent advancements in detector technology, experimentally studying CEvNS has become possible recently, as demonstrated by the COHERENT collaboration using a CsI target [3] and an Ar target [4].

2 Motivations

The discovery of CEνNS and its enhanced cross section shows potential to mitigate the elusiveness of neutrinos and therefore revolutionize their study at energies on the order of a few tens of MeV, which include geoneutrinos [5], reactor neutrinos [6], accelerator neutrinos from meson decays at rest [7-10], solar neutrinos [11], and supernova neutrino bursts [12]. Characterizing the cross section of CEν NS is also essential for dark matter searches as CEνNS constitutes an irreducible background, the so-called neutrino floor [13]. Being mediated by flavor-insensitive neutral currents, the detection of CEν NS provides extended sensitivity to sterile neutrinos [14-16] and other new physics signatures [17-20], and allows the study of the neutrino magnetic moment [21, 22], its effective charge radius [23], and the nuclear neutron form factor [24, 25]. Applications, such as deploying neutrino detectors to increase nuclear security [26, 27], might also be possible. Moreover, CEνNS is relevant to theoretical astrophysics as a key actor during stellar collapse [28-30].

3 CEνNS experiments

Because of the aforementioned findings, an increasing number of CEνNS detector technologies have been proposed [31-42], and several experiments are ongoing or have been proposed: COHERENT [43], using CsI, NaI, high-purity Ge (HPGe), and liquid-Ar targets; CONUS [44], NCC-1701 [45, 46], and νGEN [47] using cryogenic HPGe; MINER [48], using cryogenic HPGe/Si; NUCLEUS [49], using cryogenic $CaWO_4$ and Al_2O_3; CONNIE [44], using Si charge-coupled devices (CCDs); TEXONO [50], using p-type point-contact Ge; RES-NOVA, using cryogenic $PbWO_4$ [51, 52]; RICOCHET [53], using cryogenic HPGe bolometers; and RED100 [54], using liquid-Xe.

To get the most from CEνNS, an ideal detector should be inexpensive to produce and operate, have excellent energy resolutions to identify nuclear recoils with an energy of a few keV, and be made of heavy nuclear targets to exploit the quadratic scaling of the cross section. In this study, we point out, for the first time, the excellent prospects of lead perovskites to build up future CEνNS detectors and discuss their experimental feasibility in light of existing measurements.

4 Lead perovskites

Lead halide perovskites (LHPs) are novel semiconductors with exceptional optoelectronic properties, a versatile chemical composition, and low-cost synthesis. They typically consist of crystals with structure $APbX_3$, as shown in Figure 1, where A is CH_3NH_{3+} (MA^+), $CHNH_3^+$ (FA^+) or Cs^+; B is Pb^{2+}; and X is Cl^-, Br^-, and I^- [55].

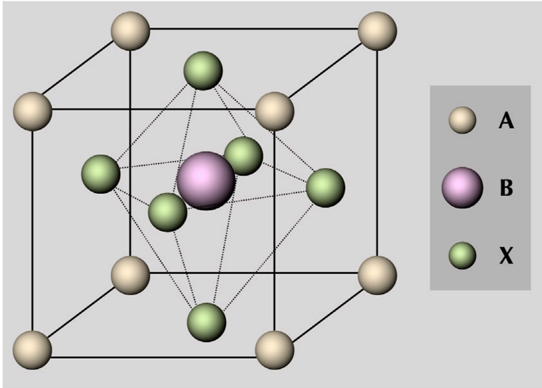

FIGURE 1
Schematic representation of the perovskite ABX_3 crystal structure.

The study of halide perovskites as photosensors was sparked about a decade ago in the context of solar cell development [56] and quickly emerged as an active field of research due to record energy conversion efficiencies [57-64]. Along the process, much has been learned about the basic properties of this material, which combines a low exciton binding energy on the order of few meV [65] with exceptionally long electron–hole diffusion lengths exceeding 1 μm [66], a tunable band gap in the range of 1.2–2.4 eV [67-68], and a high bulk resistivity of $10^{7-10}\Omega$·cm at room temperature [69]. The aforementioned combination is unique as it pairs efficient charge carrier production and mobility at a low voltage bias with a high bulk resistivity and orders of magnitude higher than those of Si and Ge, suppressing dark current and noise. Moreover, LHPs naturally allow for the manufacture of crystals with very high atomic numbers, such as $CsPbI_3$, and the design of application-specific perovskite sensors by means of stoichiometry engineering [70, 71]. Furthermore, the synthesis of LHPs is easy and flexible through techniques such as solution processing and melt growth, and single crystals with sizes > 1cm^3 can be routinely built [72]. The production cost is also low, with an estimated price of <0.3\$/cm^3 [55], namely, at a density of 4 g/cm^3 and an inexpensive cost of 75 \$/kg. Finally, LHPs can be operated inexpensively at room temperature.

5 Perovskites as radiation detectors

Lead perovskites' striking performance as solar cells and their high atomic numbers[1] quickly attracted the interest of the medical imaging community toward this material as x/γ-ray detectors [73-81]. In 2015, $MAPbI_3$ was proven to detect γ-rays from ^{137}Cs [82], and the first x-ray images were obtained [83]. Since then, a steady

1 Photon attenuation increases $\propto Z^4$, where Z is the atomic number.

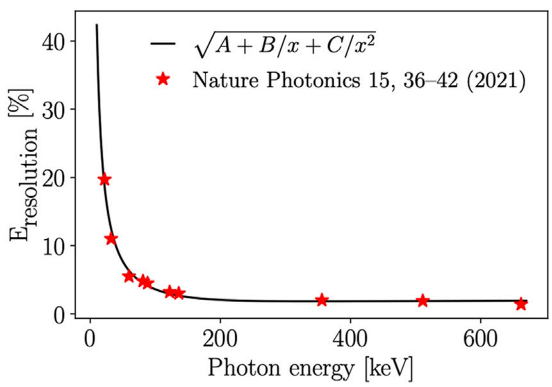

FIGURE 2
Fit to the energy resolution measured for single photons using a $CsPbBr_3$ perovskite at room temperature. Data from [95]. The best parameters are A, B, and C = {4.95, −1098.24, and 189690.18}.

improvement in x/γ-ray performance metrics and achievements has been reported over time [72, 74, 83, 84], including the best x-ray sensitivities yet achieved in any material [85, 86]. Other radiation types have also been studied with perovskites, specifically neutrons [87] and α [88, 89] and β [90] particles. For a recent review, see [91]. Moreover, perovskite nanoparticles show enormous potential as wavelength shifters, for a review see [92], making them interesting doping materials (≈1 g/L) to build nanocrystal-doped liquid scintillators, with applications in neutrino detection [93]. In this study, nevertheless, we focus on solid lead perovskite crystals as a target, i.e., a detector where 100% of the active volume is made of lead perovskite, enhancing the cross section of CEνNS enhanced due to the presence of lead. As crystals, despite the many achievements that are previously listed, all reported precision measurements involving low-energy O (10–100) keV particles have been based on the detection of recoiling electrons induced by x-ray interactions. Possibly because of this finding, no mentions exist in the literature about the possibility of measuring CEνNS using perovskites. In CEν NS, a nuclear recoil, instead of an electron recoil, needs to be measured. For Ge, it has been measured that nuclear recoils generate about a third of the ionization signal of their electronic counterparts [94]. For lead perovskites, this fraction, the so-called quenching Q, is still unknown. Quenching acts by reducing the signal, therefore, reported sensor metrics in x/γ-ray measurements that are expected to degrade when used to study CEνNS. If $Q^{\text{perovskite}} \approx Q^{\text{Ge}}$, then the energy resolution E_{res} for nuclear and electron recoils can be related by

$$E_{res}^{nuclear} \approx E_{res}^{electron} \times Q^{\text{perovskite}} \approx E_{res}^{electron} \big/ 3\,. \quad (2)$$

Existing $E_{res}^{electron}$ measurements are presented in Figure 2. These data were reported in 2021 using $CsPbBr_3$ lead perovskite crystals at room temperature [95]. A stable operation was achieved with them for over 18 months. A fit to the data smoothly reproduces the trend. Using the fit, we calculate that the energy resolution would get worse than 100% for photon energies below 4.3 keV. Taking this value as a reference to define an approximate detection threshold, Eq. 2 suggests that, if lead perovskite quenching is similar to that of Ge, existing lead perovskite sensors could have a detection threshold similar to 15 keV for nuclear recoils. Certainly, a definitive answer requires an experimental determination of $Q^{\text{perovskite}}$, a measurement that we encourage for the first time in this study. It must be emphasized that existing lead perovskite sensors are still far from their ultimate energy resolution [95], and therefore, future sensors should lead to even lower detection thresholds. Room for improvement ranges from an increase in the detected signal, e.g., reducing crystal defects [96] and improving the electrode contacts [97, 98], to a decrease in noise, e.g., passivating the sensor surfaces [99], using dopant compensation [100, 101], or operating at cryogenic temperatures. In this way, even if future measurements show that $Q^{\text{perovskite}} > Q^{\text{Ge}}$, current data and sensor improvement trends suggest that reaching O (10) keV nuclear recoil detection thresholds will likely be possible in the near future.

6 Prospects as CEνNS detectors

Producing low-activity lead perovskites should be readily possible, e.g., $CsPbI_3$ consists of Cs and I, both used in the first historical detection of CEνNS [3], and archaeological Pb has recently been demonstrated to be adequate for CEνNS detection [102]. Moreover, $CsPbI_3$ and other lead perovskites are made up of strikingly heavy elements, significantly advantaging the CEνNS interaction cross section of mainstream alternative materials and, in particular, that of Ge. However, the maximum recoil energy decreases linearly with m_N, and therefore, the ability of the detector to identify the recoiling nucleus needs to be considered. To account for it, we define the effective cross section, σ_{eff}, as a figure of merit, defined as

$$\sigma_{\text{eff}} \equiv \int_{E^{\text{recoil}}_{\text{threshold}}}^{E_R^{\max}} \frac{d\sigma}{dE_R}\, \epsilon \, dE_R \quad (3)$$

which can be calculated from Eq. 1 if the detector efficiency, ϵ, is specified. Using it, in Figure 3 $CsPbI_3$ and Ge targets[2] are directly compared for some neutrino energies, assuming a detector with perfect (null) efficiency above (below) a certain energy recoil threshold, $E^{\text{recoil}}_{\text{threshold}}$.

If, as suggested in the previous section, $E^{\text{recoil}}_{\text{threshold}} \approx 15$ keV in existing lead perovskite sensors, studying 30–50 MeV neutrinos could be readily possible. Interestingly, this neutrino energy range overlaps with the energy spectrum of neutrinos produced in pion decay at rest (π-DAR) neutrino sources [103, 104]. π-DAR neutrinos have been used in the only two CEνNS measurements so far, using 14.6 kg of CsI [3] and 24 kg of argon [4]. Building and operating similar masses of lead perovskite poses no apparent impediment, with the driving cost being the number of electronic channels. If sensor masses similar to 1 g are deployed, a reasonable and potentially scalable $O\ (10^4)$ number of electronic channels would be needed to set up the experiment. CEνNS experiments at π-DAR sources are primarily counting

2 For $CsPbI_3$, the weighted average (Cs + Pb+3I)/5 is used in the result of Eq. 3.

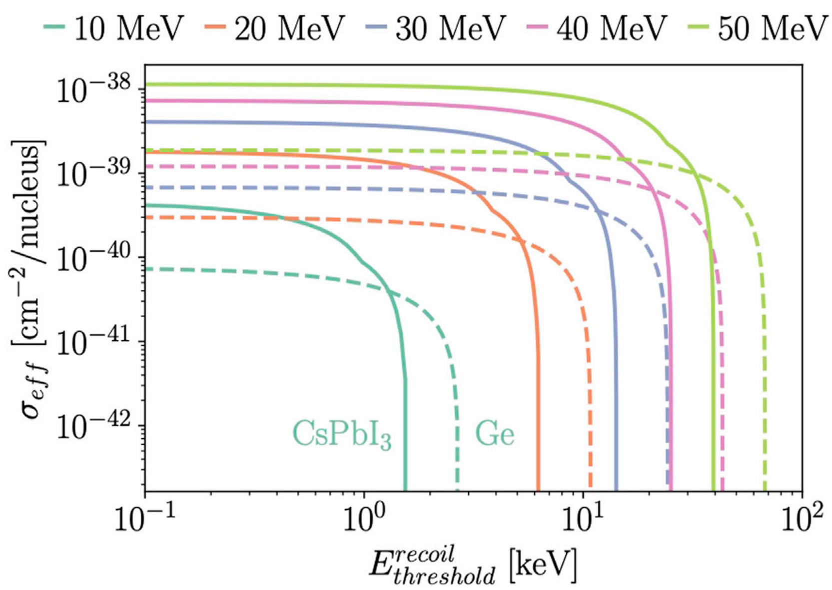

FIGURE 3
CE$\bar{\nu}$NS interaction cross section per nucleus, σ, multiplied by the detector efficiency, ϵ, as a function of the recoil energy threshold, $E^{\text{recoil}}_{\text{threshold}}$. Solid (dashed) lines correspond to $CsPbI_3$ (Ge).

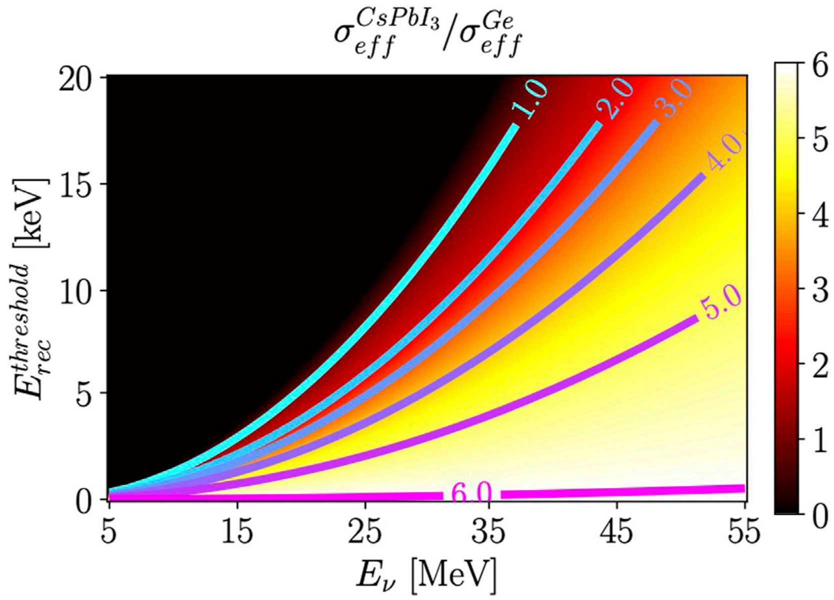

FIGURE 4
The color map depicts the ratio of $\sigma^{CsPbI_3}_{\text{eff}}/\sigma^{Ge}_{\text{eff}}$ as a function of the neutrino energy, E_ν, and the recoil energy threshold, $E^{\text{recoil}}_{\text{threshold}}$. A ratio value of zero indicates that $E^{\text{recoil}}_{\text{threshold}}$ is above the necessary level to observe any recoil in $CsPbI_3$. To help the visualization, values of some particular integer ratios are highlighted by color lines.

experiments that observe the event rate variation induced by switching on and off the neutrino beam, allowing to characterize the background levels and cancel out effects related to the detector efficiency. Neutrino energy is not reconstructed. Instead, the measurement observable is directly the reconstructed signal distribution above the detection threshold (see, for instance, [3]). Signal interactions are contained in individual sensors, and therefore, no spatial resolution is needed. If the detector is deployed as a dense array of lead perovskite sensors, identifying nearby sensor coincidences could be used to assist auxiliary veto modules to reject the background.

The comparison between $CsPbI_3$ and Ge in Figure 3 reflects that for a given fixed neutrino energy, lead perovskites require a smaller $E^{recoil}_{threshold}$ to observe CEνNS. However, if the detection threshold is achieved and mildly lowered, it results in a large enhancement of the interaction cross section. This trade-off is characterized by the ratio $\sigma^{CsPbI_3}_{eff}/\sigma^{Ge}_{eff}$ presented in Figure 4. For $E^{recoil}_{threshold} \approx 15$ keV, as previously suggested, Ge and $CsPbI_3$ would lead to similar event rates for π-DAR neutrinos. However, although the fabrication and operation of Ge sensors are nearly optimal, perovskite R&D shows potential to lower its $E^{recoil}_{threshold}$ in the next few years, resulting in an up to six-fold event rate increase compared to Ge. Moreover, such a detection improvement would also open the door to investigating the use of lead perovskites to measure neutrinos from other sources, e.g., supernova and reactor neutrinos. Lastly, perovskites are orders of magnitude cheaper to manufacture and potentially operate[3] than existing alternatives, including HPGe.

7 Discussion and outlook

In just one decade, lead perovskites have been established as novel materials with transformative potential as radiation detectors due to their unique optoelectronic properties.

In this study, we highlight their potential as neutrino detector targets and discussed, for the first time, their suitability for the study of CEνNS. In particular, we note that existing x-ray data indicate that current lead perovskites sensors might already be suitable to study π-DAR neutrinos and discuss their implications. In general, with the available data, no impediments are apparent that prevent further development of the concept of lead perovskites for neutrino detection. Nonetheless, we highlight the necessity of determining the quenching fraction for recoiling the nucleus in lead perovskites to evaluate its exact effect. In any case, to bring perovskites to their ultimate detection potential and enable their full range of applications, active R&D is required. In particular, efforts to optimize lead perovskite sensors for the detection of single low-energy particles would be significantly beneficial for the development of this technology within the field of experimental neutrino physics.

Lastly, we note that CEνNS and some dark-matter models share the same signal mechanism, i.e., the detection of nuclear recoils. Therefore, any progress in this direction might benefit both the neutrino and dark-matter research communities.

3 Perovskites might be able to operate without the need for cryogenic systems, as supported by existing x-ray data.

Data availability statement

The original contributions presented in the study are included in the article/Supplementary Material; further inquiries can be directed to the corresponding authors.

Author contributions

CJ-V and FS contributed to the conception and design of the study. CJ-V performed the cross section calculations. CJ-V wrote the first draft of the manuscript. CJ-V and FS wrote sections of the manuscript. All authors contributed to the article and approved the submitted version.

Funding

This project was partially inspired by the ZPro project funded by the Barcelona Institute of Technology (BIST). Open access funding was provided by the University of Geneva.

Acknowledgments

The authors acknowledge fruitful discussions with E. Palomares and valuable feedback from J. I. Collar and L. Pattavina.

Conflict of interest

The authors declare that the research was conducted in the absence of any commercial or financial relationships that could be construed as a potential conflict of interest.

Publisher's note

References

1. Freedman DZ. Coherent effects of a weak neutral current. *Phys Rev D* (1974) 9: 1389–92. doi:10.1103/physrevd.9.1389

2. Scholberg K. Coherent elastic neutrino-nucleus scattering. *J Phys Conf Ser* (2020) 1468:012126. doi:10.1088/1742-6596/1468/1/012126

3. Akimov D, Albert JB, An P, Awe C, Barbeau PS, Becker B, et al. Observation of coherent elastic neutrino-nucleus scattering. *Science* (2017) 357:1123. (COHERENT) arXiv:1708.01294 [nucl-ex].

4. Akimov D, Albert JB, An P, Awe C, Barbeau PS, Becke B, et al. First measurement of coherent elastic neutrino-nucleus scattering on argon. *Phys Rev Lett* (2021) 126: 012002. (COHERENT) arXiv:2003.10630 [nucl-ex]. doi:10.1103/PhysRevLett.126.012002

5. Sramek O, McDonough WF, Kite ES, Lekic V, Dye S, Zhong S. Geophysical and geochemical constraints on geoneutrino fluxes from Earth's mantle. *Earth Planet Sci Lett* (2013) 361:356–66. arXiv:1207.0853 [physics.geo-ph]. doi:10.1016/j.epsl.2012.11.001

6. Qian X, Peng JC. Physics with reactor neutrinos. *Rept Prog Phys* (2019) 82:036201. arXiv:1801.05386 [hep-ex]. doi:10.1088/1361-6633/aae881

7. Ajimura S, Cheoun MK, Choi JH, Furuta H, Harada M, Hasegawa S, et al. *Technical design report (TDR): searching for a sterile neutrino at J-PARC MLF (E56, JSNS2)* (2017). arXiv:1705.08629 [physics.ins-det].

8. Garoby R, Vergara A, Danared H, Alonso I, Bargallo E, Cheymol B, et al. The European spallation source design. *Phys Scripta* (2018) 93:014001. doi:10.1088/1402-4896/aa9bff

9. Wang F, Liang T, Yin W, Yu Q, He L, Tao J, et al. Physical design of target station and neutron instruments for China Spallation Neutron Source. *Sci China Phys Mech Astron* (2013) 56:2410–24. doi:10.1007/s11433-013-5345-5

10. Alonso J, Avignone FT, Barletta WA, Barlow R, Baumgartner HT. *Expression of interest for a novel search for CP violation in the neutrino sector: DAEdALUS* (2010). arXiv:1006.0260 [physics.ins-det].

11. Bahcall JN, Pinsonneault MH, Basu S. Solar models: Current epoch and time dependences, neutrinos, and helioseismological properties. *Astrophys J* (2001) 555: 990–1012. arXiv:astro-ph/0010346. doi:10.1086/321493

12. Burrows A, Vartanyan D. Core-collapse supernova explosion theory. *Nature* (2021) 589:29–39. arXiv:2009.14157 [astro-ph.SR]. doi:10.1038/s41586-020-03059-w

13. Billard J, Strigari L, Figueroa-Feliciano E. Implication of neutrino backgrounds on the reach of next generation dark matter direct detection experiments. *Phys Rev D* (2014) 89:023524. arXiv:1307.5458 [hep-ph]. doi:10.1103/physrevd.89.023524

14. Anderson AJ, Conrad JM, Figueroa-Feliciano E, Ignarra C, Karagiorgi G, Scholberg K, et al. Measuring active-to-sterile neutrino oscillations with neutral current coherent neutrino-nucleus scattering. *Phys Rev D* (2012) 86:013004. arXiv: 1201.3805 [hep-ph]. doi:10.1103/physrevd.86.013004

15. Dutta B, Gao Y, Mahapatra R, Mirabolfathi N, Strigari LE, Walker JW, et al. Sensitivity to oscillation with a sterile fourth generation neutrino from ultralow threshold neutrino-nucleus coherent scattering. *Phys Rev D* (2016) 94:093002. arXiv: 1511.02834 [hep-ph]. doi:10.1103/physrevd.94.093002

16. Kosmas TS, Papoulias DK, Tortola M, Valle JWF. Probing light sterile neutrino signatures at reactor and Spallation Neutron Source neutrino experiments. *Phys Rev D* (2017) 96:063013. arXiv:1703.00054 [hep-ph]. doi:10.1103/physrevd.96.063013

17. Krauss LM. Low-energy neutrino detection and precision tests of the standard model. *Phys Lett B* (1991) 269:407–11. doi:10.1016/0370-2693(91)90192-s

18. Barranco J, Miranda OG, Rashba TI. Sensitivity of low energy neutrino experiments to physics beyond the standard model. *Phys Rev D* (2007) 76:073008. arXiv:hep-ph/0702175. doi:10.1103/physrevd.76.073008

19. deNiverville P, Pospelov M, Ritz A. Light new physics in coherent neutrino-nucleus scattering experiments. *Phys Rev D* (2015) 92:095005. arXiv:1505.07805 [hep-ph]. doi:10.1103/physrevd.92.095005

20. Dutta B, Mahapatra R, Strigari LE, Walker JW. Sensitivity toZ-prime and nonstandard neutrino interactions from ultralow threshold neutrino-nucleus coherent scattering. *Phys Rev D* (2016) 93:013015. arXiv:1508.07981 [hep-ph]. doi:10.1103/physrevd.93.013015

21. Dodd AC, Papageorgiu E, Ranfone S. The effect of a neutrino magnetic moment on nuclear excitation processes. *Phys Lett B* (1991) 266:434–8. doi:10.1016/0370-2693(91)91064-3

22. Kosmas TS, Miranda OG, Papoulias DK, Tortola M, Valle JWF. Probing neutrino magnetic moments at the Spallation Neutron Source facility. *Phys Rev D* (2015) 92: 013011. arXiv:1505.03202 [hep-ph]. doi:10.1103/physrevd.92.013011

23. Papavassiliou J, Bernabeu J, Passera M. Neutrino-nuclear coherent scattering and the effective neutrino charge radius. *PoS* (2006) 192. HEP2005 arXiv:hep-ph/0512029. doi:10.48550/arXiv.hep-ph/0512029

24. Patton K, Engel J, McLaughlin GC, Schunck N. Neutrino-nucleus coherent scattering as a probe of neutron density distributions. *Phys Rev C* (2012) 86:024612. arXiv:1207.0693 [nucl-th]. doi:10.1103/physrevc.86.024612

25. Amanik PS, McLaughlin GC. Nuclear neutron form factor from neutrino–nucleus coherent elastic scattering. *J Phys G* (2009) 36:015105. doi:10.1088/0954-3899/36/1/015105

26. Stewart C, Abou-Jaoude A, Erickson A. Employing antineutrino detectors to safeguard future nuclear reactors from diversions. *Nat Commun* (2019) 10:3527. doi:10.1038/s41467-019-11434-z

27. Bernstein A, Bowden N, Goldblum BL, Huber P, Jovanovic I, Mattingly J. *Colloquium*: Neutrino detectors as tools for nuclear security. *Rev Mod Phys* (2020) 92:011003. arXiv:1908.07113 [physics.soc-ph]. doi:10.1103/revmodphys.92.011003

28. Wilson JR. Coherent neutrino scattering and stellar collapse. *Phys Rev Lett* (1974) 32:849–52. doi:10.1103/physrevlett.32.849

29. Schramm DN, Arnett WD. Neutral currents and supernovas. *Phys Rev Lett* (1975) 34:113–6. doi:10.1103/physrevlett.34.113

30. Freedman DZ, Schramm DN, Tubbs DL. The weak neutral current and its effects in stellar collapse. *Ann Rev Nucl Part Sci* (1977) 27:167–207. doi:10.1146/annurev.ns.27.120177.001123

31. Drukier A, Stodolsky L. Principles and applications of a neutral-current detector for neutrino physics and astronomy. *Phys Rev D* (1984) 30:2295–309. doi:10.1103/physrevd.30.2295

32. Cabrera B, Krauss LM, Wilczek F. Bolometric detection of neutrinos. *Phys Rev Lett* (1985) 55:25–8. doi:10.1103/physrevlett.55.25

33. Formaggio JA, Figueroa-Feliciano E, Anderson AJ. Sterile neutrinos, coherent scattering, and oscillometry measurements with low-temperature bolometers. *Phys Rev D* (2012) 85:013009. arXiv:1107.3512 [hep-ph]. doi:10.1103/physrevd.85.013009

34. Braggio C, Bressi G, Carugno G, Feltrin E, Galeazzi G. Massive silicon or germanium detectors at cryogenic temperature. *Nucl Instrum Meth A* (2006) 568: 412–5. doi:10.1016/j.nima.2006.06.008

35. Barbeau PS, Collar JI, Tench O. Large-mass ultralow noise germanium detectors: performance and applications in neutrino and astroparticle physics. *JCAP* (2007) 09: 009. arXiv:nucl-ex/0701012. doi:10.1088/1475-7516/2007/09/009

36. Fernandez Moroni G, Estrada J, Paolini EE, Cancelo G, Tiffenberg J, Molina J. Charge coupled devices for detection of coherent neutrino-nucleus scattering. *Phys Rev D* (2015) 91:072001. arXiv:1405.5761 [physics.ins-det]. doi:10.1103/physrevd.91.072001

37. Horowitz CJ, Coakley KJ, McKinsey DN. Supernova observation via neutrino-nucleus elastic scattering in the CLEAN detector. *Phys Rev D* (2003) 68:023005. arXiv: astro-ph/0302071. doi:10.1103/physrevd.68.023005

38. Bondar A, Buzulutskov A, Grebenuk A, Pavlyuchenko D, Snopkov R, Tikhonov Y, et al. A two-phase argon avalanche detector operated in a single electron counting mode. *Nucl Instrum Meth A* (2007) 574:493–9. arXiv:physics/0611068. doi:10.1016/j.nima.2007.01.090

39. Joshi TH, Sangiorgio S, Bernstein A, Foxe M, Hagmann C, Jovanovic I, et al. First measurement of the ionization yield of nuclear recoils in liquid argon, *Phys Rev Lett* (2014) 112:171303. arXiv:1402.2037 [physics.ins-det]. 10.1103/PhysRevLett.112.171303.

40. Akimov DY, Alexandrov IS, Aleshin VI, Belov VA, Bolozdynya AI, Burenkov AA, et al. Prospects for observation of neutrino-nuclear neutral current coherent scattering with two-phase Xenon emission detector. *JINST* (2013) 8:P10023. arXiv: 1212.1938 [physics.ins-det]. doi:10.1088/1748-0221/8/10/P10023

41. Brice SJ, Cooper RL, DeJongh F, Empl A, Garrison LM, Hime A, et al. A new method for measuring coherent elastic neutrino nucleus scattering at an off-Axis high-energy neutrino beam target. *Phys Rev D* (2014) 89:072004. arXiv: 1311.5958 [physics.ins-det]. doi:10.1103/PhysRevD.89.072004

42. Collar JI, Fields NE, Hai M, Hossbach TW, Orrell JL, Overman CT, et al. Coherent neutrino-nucleus scattering detection with a CsI[Na] scintillator at the SNS spallation source. *Nucl Instrum Meth A* (2015) 773:56–65. arXiv:1407.7524 [physics.ins-det]. doi:10.1016/j.nima.2014.11.037

43. Akimov D, An P, Awe C, Barbeau PS, Barton P, Becker B, et al. "*The COHERENT experiment at the spallation neutron source* (2015). (COHERENT) arXiv: 1509.08702 [physics.ins-det].

44. Aguilar-Arevalo A, Bertou X, Bonifazi C, Butner M, Cancelo G, Castaneda Vazquez A, et al. The CONNIE experiment. *J Phys Conf Ser* (2016) 761:012057. arXiv: 1608.01565 [physics.ins-det]. doi:10.1088/1742-6596/761/1/012057

45. Colaresi J, Collar JI, Hossbach TW, Kavner ARL, Lewis CM, Robinson AE, et al. First results from a search for coherent elastic neutrino-nucleus scattering at a reactor site. *Phys Rev D* (2021) 104:072003. arXiv:2108.02880 [hep-ex]. doi:10.1103/physrevd.104.072003

46. Colaresi J, Collar JI, Hossbach TW, Lewis CM, Yocum KM. Measurement of coherent elastic neutrino-nucleus scattering from reactor antineutrinos. *Phys Rev Lett* (2022) 129:211802. arXiv:2202.09672 [hep-ex]. doi:10.1103/physrevlett.129.211802

47. Belov V, Brudanin V, Egorov V, Filosofov D, Fomina M, Gurov Y, et al. The νGeN experiment at the kalinin nuclear power plant. *JINST* (2015) 10:P12011. doi:10.1088/1748-0221/10/12/p12011

48. Agnolet G, Baker W, Barker D, Beck R, Carroll TJ, Cesar J, et al. Background studies for the MINER coherent neutrino scattering reactor experiment. *Nucl Instrum Meth A* (2017) 853:53. (MINER) arXiv:1609.02066 [physics.ins-det]. doi:10.48550/arXiv.1609.02066

49. Strauss R, Rothe J, Angloher G, Bento A, Gütlein A, Hauff D, et al. The ν-cleus experiment: a gram-scale fiducial-volume cryogenic detector for the first detection of coherent neutrino-nucleus scattering. *Eur Phys J C* (2017) 77:506. arXiv: 1704.04320 [physics.ins-det]. doi:10.1140/epjc/s10052-017-5068-2

50. Singh L, Wong HT. Low energy neutrino physics with sub-keV Ge-detectors at kuo-sheng neutrino laboratory. *J Phys Conf Ser* (2017) 888:012124. TEXONO. doi:10.1088/1742-6596/888/1/012124

51. Pattavina L, Ferreiro Iachellini N, Tamborra I. Neutrino observatory based on archaeological lead. *Phys Rev D* (2020) 102:063001. arXiv:2004.06936 [astro-ph.HE]. doi:10.1103/physrevd.102.063001

52. Ferreiro Iachellini N, Pattavina L, Abdelhameed AH, Bento A, Canonica L, Danevich F, et al. Operation of an archaeological lead PbWO$$_4$$ crystal to search for neutrinos from astrophysical sources with a transition edge sensor. *J Low Temp Phys* (2022) 209:872–8. arXiv:2111.07638 [physics.ins-det]. doi:10.1007/s10909-022-02823-8

53. Augier C, Beaulieu G, Belov V, Berge L, Billard J, Bres G, et al. Ricochet progress and status. *J. Low Temp. Phys.* (2023) 212:127–137. doi:10.1007/s10909-023-02971-5

54. Akimov DY, Belov V, Bolozdynya A, Dolgolenko A, Efremenko Y, Etenko A, et al. First ground-level laboratory test of the two-phase xenon emission detector RED-100. *JINST* (2020) 15:P02020. arXiv:1910.06190 [physics.ins-det]. doi:10.1088/1748-0221/15/02/p02020

55. Wei H, Huang J. Halide lead perovskites for ionizing radiation detection. *Nat Commun* (2019) 10:1.

56. Kojima A, Teshima K, Shirai Y, Miyasaka T. Organometal halide perovskites as visible-light sensitizers for photovoltaic cells. *J Am Chem Soc* (2009) 131:6050–1. doi:10.1021/ja809598r

57. Green MA, Ho-Baillie A, Snaith HJ. The emergence of perovskite solar cells. *Nat Photon* (2014) 8:506–14. doi:10.1038/nphoton.2014.134

58. Jung HS, Park NG. Perovskite solar cells: from materials to devices. *small* (2015) 11:10–25. doi:10.1002/smll.201402767

59. Park NG. Perovskite solar cells: An emerging photovoltaic technology. *Mater Today* (2015) 18:65–72. doi:10.1016/j.mattod.2014.07.007

60. Correa-Baena J-P, Saliba M, Buonassisi T, Grätzel M, Abate A, Tress W, et al. Promises and challenges of perovskite solar cells. *Science* (2017) 358:739–44. doi:10.1126/science.aam6323

61. Huang J, Yuan Y, Shao Y, Yan Y. Understanding the physical properties of hybrid perovskites for photovoltaic applications. *Nat Rev Mater* (2017) 2:1.

62. Yang D, Yang R, Wang K, Wu C, Zhu X, Feng J, et al. High efficiency planar-type perovskite solar cells with negligible hysteresis using EDTA-complexed SnO2. *Nat Commun* (2018) 9:1. doi:10.1038/s41467-018-05760-x

63. Kim JY, Lee J-W, Jung HS, Shin H, Park NG. High-efficiency perovskite solar cells. *Chem Rev* (2020) 120:7867–918. doi:10.1021/acs.chemrev.0c00107

64. Yoo JJ, Seo G, Chua MR, Park TG, Lu Y, Rotermund F, et al. Efficient perovskite solar cells via improved carrier management. *Nature* (2021) 590:587–93. doi:10.1038/s41586-021-03285-w

65. Miyata A, Mitioglu A, Plochocka P, Portugall O, Wang JT-W, Stranks SD, et al. Direct measurement of the exciton binding energy and effective masses for charge carriers in organic–inorganic tri-halide perovskites. *Nat Phys* (2015) 11:582–7. doi:10.1038/nphys3357

66. Stranks SD, Eperon GE, Grancini G, Menelaou C, Alcocer MJ, Leijtens T, et al. Electron-hole diffusion lengths exceeding 1 micrometer in an organometal trihalide perovskite absorber. *Science* (2013) 342:341–4. doi:10.1126/science.1243982

67. Ju D, Dang Y, Zhu Z, Liu H, Chueh C-C, Li X, et al. Tunable band gap and long carrier recombination lifetime of stable mixed $CH_3NH_3Pb_xSn_{1-x}Br_3$ single crystals. *Chem Mater* (2018) 30:1556–65. doi:10.1021/acs.chemmater.7b04565

68. Unger E, Kegelmann L, Suchan K, Sörell D, Korte L, Albrecht S. Roadmap and roadblocks for the band gap tunability of metal halide perovskites. *J Mater Chem A* (2017) 5:11401–9. doi:10.1039/c7ta00404d

69. Pisoni A, Jacimovic J, Barisic OS, Spina M, Gaál R, Forró L, et al. Ultra-low thermal conductivity in organic–inorganic hybrid perovskite $CH_3NH_3PbI_3$. *J Phys Chem Lett* (2014) 5:2488–92. doi:10.1021/jz5012109

70. Emara J, Schnier T, Pourdavoud N, Riedl T, Meerholz K, Olthof S. Impact of film stoichiometry on the ionization energy and electronic structure of $CH_3NH_3PbI_3$Perovskites. *Adv Mater* (2016) 28:553–9. doi:10.1002/adma.201503406

71. Xiao Y, Jia S, Bu N, Li N, Liu Y, Liu M, et al. Grain and stoichiometry engineering for ultra-sensitive perovskite X-ray detectors. *J Mater Chem A* (2021) 9:25603–10. doi:10.1039/d1ta07585c

72. He Y, Matei L, Jung HJ, McCall KM, Chen M, Stoumpos CC, et al. High spectral resolution of gamma-rays at room temperature by perovskite CsPbBr3 single crystals. *Nat Commun* (2018) 9:1. doi:10.1038/s41467-018-04073-3

73. Shrestha S, Fischer R, Matt GJ, Feldner P, Michel T, Osvet A, et al. High-performance direct conversion X-ray detectors based on sintered hybrid lead triiodide perovskite wafers. *Nat Photon* (2017) 11:436–40. doi:10.1038/nphoton.2017.94

74. Wei W, Zhang Y, Xu Q, Wei H, Fang Y, Wang Q, et al. Monolithic integration of hybrid perovskite single crystals with heterogenous substrate for highly sensitive X-ray imaging. *Nat Photon* (2017) 11:315–21. doi:10.1038/nphoton.2017.43

75. Kim YC, Kim KH, Son D-Y, Jeong D-N, Seo J-Y, Choi YS, et al. Printable organometallic perovskite enables large-area, low-dose X-ray imaging. *Nature* (2017) 550:87–91. doi:10.1038/nature24032

76. García de Arquer FP, Armin A, Meredith P, Sargent EH. Solution-processed semiconductors for next-generation photodetectors. *Nat Rev Mater* (2017) 2:1. doi:10.1038/natrevmats.2016.100

77. Gill HS, Elshahat B, Kokil A, Li L, Mosurkal R, Zygmanski P, et al. Flexible perovskite based X-ray detectors for dose monitoring in medical imaging applications. *Phys Med* (2018) 5:20–3. doi:10.1016/j.phmed.2018.04.001

78. Zhuang R, Wang X, Ma W, Wu Y, Chen X, Tang L, et al. Highly sensitive X-ray detector made of layered perovskite-like (NH4)3Bi2I9 single crystal with anisotropic response. *Nat Photon* (2019) 13:602–8. doi:10.1038/s41566-019-0466-7

79. Zhou F, Li Z, Lan W, Wang Q, Ding L, Jin Z. Halide perovskite, a potential scintillator for X-ray detection. *Small Methods* (2020) 4:2000506. doi:10.1002/smtd.202000506

80. Li X, Meng C, Huang B, Yang D, Xu X, Zeng H. All-perovskite integrated X-ray detector with ultrahigh sensitivity. *Adv Opt Mater* (2020) 8:2000273. doi:10.1002/adom.202000273

81. Su Y, Ma W, Yang YM. Perovskite semiconductors for direct X-ray detection and imaging. *J Semiconductors* (2020) 41:051204. doi:10.1088/1674-4926/41/5/051204

82. Dong Q, Fang Y, Shao Y, Mulligan P, Qiu J, Cao L, et al. Electron-hole diffusion lengths > 175 μm in solution-grown $CH_3NH_3PbI_3$ single crystals. *Science* (2015) 347:967–70. doi:10.1126/science.aaa5760

83. Yakunin S, Sytnyk M, Kriegner D, Shrestha S, Richter M, Matt GJ, et al. Detection of X-ray photons by solution-processed lead halide perovskites. *Nat Photon* (2015) 9:444–9. doi:10.1038/nphoton.2015.82

84. Wei H, Fang Y, Mulligan P, Chuirazzi W, Fang H-H, Wang C, et al. Sensitive X-ray detectors made of methylammonium lead tribromide perovskite single crystals. *Nat Photon* (2016) 10:333–9. doi:10.1038/nphoton.2016.41

85. Jiang J, Xiong M, Fan K, Bao C, Xin D, Pan Z, et al. Synergistic strain engineering of perovskite single crystals for highly stable and sensitive X-ray detectors with low-bias imaging and monitoring. *Nat Photon* (2022) 16:575–81. doi:10.1038/s41566-022-01024-9

86. He Y, Hadar I, De Siena MC, Klepov VV, Pan L, Chung DY, et al. Sensitivity and detection limit of spectroscopic-grade perovskite CsPbBr3 crystal for hard X-ray detection. *Adv Funct Mater* (2022) 32:2112925. doi:10.1002/adfm.202112925

87. Andričević P, Náfrádi G, Kollár M, Náfrádi B, Lilley S, Kinane C, et al. Hybrid halide perovskite neutron detectors. *Scientific Rep* (2021) 11:1.

88. He Y, Liu Z, McCall KM, Lin W, Chung DY, Wessels BW, et al. Perovskite CsPbBr3 single crystal detector for alpha-particle spectroscopy. *Nucl Instr Methods Phys Res Section A: Acc Spectrometers, Detectors Associated Equipment* (2019) 922:217–21. doi:10.1016/j.nima.2019.01.008

89. Xie A, Hettiarachchi C, Maddalena F, Witkowski ME, Makowski M, Drozdowski W, et al. Lithium-doped two-dimensional perovskite scintillator for wide-range radiation detection. *Commun Mater* (2020) 1:37. doi:10.1038/s43246-020-0038-x

90. Yu D, Wang P, Cao F, Gu Y, Liu J, Han Z, et al. Two-dimensional halide perovskite as β-ray scintillator for nuclear radiation monitoring. *Nat Commun* (2020) 11:3395. doi:10.1038/s41467-020-17114-7

91. Liu F, Wu R, Zeng Y, Wei J, Li H, Manna L, et al. Halide perovskites and perovskite related materials for particle radiation detection. *Nanoscale* (2022) 14:6743–60. doi:10.1039/d2nr01292h

92. Dey A, Ye J, De A, Debroye E, Ha SK, Bladt E, et al. State of the art and prospects for halide perovskite nanocrystals. *ACS nano* (2021) 15:10775–981. doi:10.1021/acsnano.0c08903

93. Graham E, Gooding D, Gruszko J, Grant C, Naranjo B, Winslow L. Light yield of Perovskite nanocrystal-doped liquid scintillator. *JINST* (2019) 14:P11024. doi:10.1088/1748-0221/14/11/p11024

94. Martineau O, Benoit A, Bergé L, Broniatowski A, Chabert L, Chambon B, et al. Calibration of the EDELWEISS cryogenic heat-and-ionization germanium detectors for dark matter search. *Nucl Instrum Meth A* (2004) 530:426. arXiv:astro-ph/0310657.

95. He Y, Petryk M, Liu Z, Chica DG, Hadar I, Leak C, et al. CsPbBr3 perovskite detectors with 1.4% energy resolution for high-energy γ-rays. *Nat Photon* (2021) 15:36–42. doi:10.1038/s41566-020-00727-1

96. Pan Z, Wu L, Jiang J, Shen L, Yao K. Searching for high-quality halide perovskite single crystals toward X-ray detection. *J Phys Chem Lett* (2022) 13:2851–61. doi:10.1021/acs.jpclett.2c00450

97. Aranda C, Bisquert J, Guerrero A. Impedance spectroscopy of perovskite/contact interface: Beneficial chemical reactivity effect. *J Chem Phys* (2019) 151:124201. doi:10.1063/1.5111925

98. Lin C-H, Hu L, Guan X, Kim J, Huang C-Y, Huang J-K, et al. Electrode engineering in halide perovskite electronics: Plenty of room at the interfaces. *Adv Mater* (2022) 34:2108616. doi:10.1002/adma.202108616

99. Song Y, Li L, Bi W, Hao M, Kang Y, Wang A, et al. Atomistic surface passivation of $CH_3NH_3PbI_3$ perovskite single crystals for highly sensitive coplanar-structure X-ray detectors. *Research* (2020) 2020:5958243. doi:10.34133/2020/5958243

100. Wei H, DeSantis D, Wei W, Deng Y, Guo D, Savenije TJ, et al. Dopant compensation in alloyed CH3NH3PbBr3−xClx perovskite single crystals for gamma-ray spectroscopy. *Nat Mater* (2017) 16:826–33. doi:10.1038/nmat4927

101. Wu J, Wang L, Feng A, Yang S, Li N, Jiang X, et al. Self-powered $FA_{0.55}MA_{0.45}PbI_3$ single-crystal perovskite X-ray detectors with high sensitivity. *Adv Funct Mater* (2022) 32:2109149. doi:10.1002/adfm.202109149

102. Beeman JW, Benato G, Bucci C, Canonica L, Carniti P, Celi E, et al. Characterization of a kg-scale archaeological lead-based cryogenic detectors for the RES-NOVA experiment. *Appl Radiat Isot* (2023) 194:110704. arXiv:2206.05116 [physics.ins-det]. doi:10.48550/arXiv.2206.05116

103. Akimov D, An P, Awe C, Barbeau PS, Becke B, Belov V, et al. Simulating the neutrino flux from the spallation neutron source for the COHERENT experiment. *Phys Rev D* (2022) 106:032003. COHERENT arXiv:2109.11049 [hep-ex].

104. Barbeau PS, Efremenko Y, Scholberg K. *COHERENT at the spallation neutron source* (2021). arXiv:2111.07033 [hep-ex].